JOC Article
pubs.acs.org/joc

Substitutent Effects in the Periphery of 2,9-Bisaryl-tetraazaperopyrene Dyes

Susanne C. Martens, Till Riehm, Sonja Geib, Hubert Wadepohl, and Lutz H. Gade*

Anorganisch-Chemisches Institut, Universität Heidelberg, Im Neuenheimer Feld 270, 69120 Heidelberg, Germany

lutz.gade@uni-hd.de

Received October 29, 2010

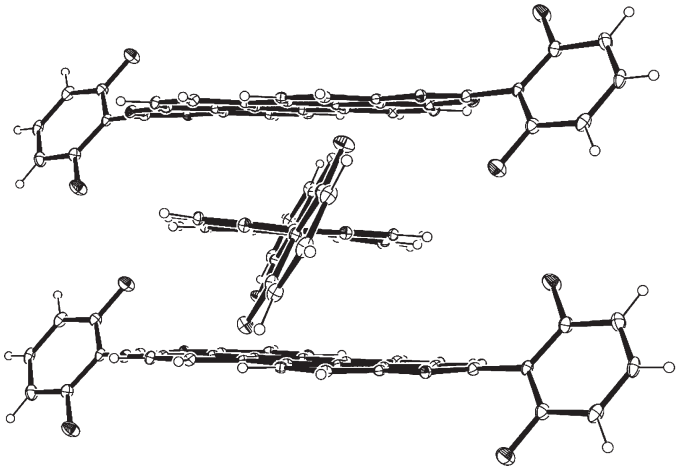

A series of 2,9-bisaryl-1,3,8,10-tetraazaperopyrene (**TAPP**) derivatives has been synthesized by reacting 4,9-diamino-3,10-perylenequinone diimine with a large excess of the corresponding benzoyl chloride in refluxing nitrobenzene. Among all derivatives only *ortho*-substituted phenyl congeners were sufficiently soluble for studying solutions of defined concentration in organic solvents. The molecular structures of the crystallized compounds, determined by X-ray diffraction of four derivatives, are determined by the planar tetraazaperopyrene core and the interplanar angle of the phenyl rings, which depends on the size of the *ortho* substituent (40−70°). The intermolecular packing pattern of all compounds is characterized by parallel stacks of molecules with the substituted phenyl rings rotated out of the peropyrene plane to reduce the steric repulsion. Crystals of a **TAPP** derivative suitable for X-ray diffraction were grown from trifluoroacetic acid (TFA) for the first time, establishing a 2-fold protonated species. The ground-state geometries of the **TAPP** derivatives were calculated by DFT [B3PW91/6-31g(d,p)] and the lowest unoccupied molecular orbital (LUMO) energies of derivatives possessing electron-withdrawing groups were decreased, as were the computed electron affinities. The results of the modeling study were confirmed experimentally by cyclic voltammetry to evaluate the substituent effects on the highest occupied molecular orbital (HOMO) and the LUMO of the peropyrene core. The UV−vis absorption spectra of all compounds recorded in trifluoroacetic acid are almost superimposable and display a characteristic visible absorption band between 460 and 490 nm (log ε = 4.64−5.01) with a strong vibrational progression of 1173−1475 cm^{-1}. Their fluorescence spectra are characterized by bands between 490 and 530 nm that are the mirror images of the absorption spectra (Stokes shifts of 10−50 nm). The luminescence quantum yields range from <0.01 to 0.30, thereby indicating a quenching effect for some substitution patterns.

Introduction

Recently, there has been a resurgence in interest in the chemistry of polycyclic aromatic hydrocarbons (PAHs)[1] due to their manifold applications in electronic and optoelectronic devices, such as light-emitting diodes, field-effect transistors (FETs), and solar cells.[2−4] The work reported herein is concerned with a new polyheterocyclic class of aromatics derived from the peropyrene family in which four of the CH groups of the heptacyclic

(1) (a) Harvey, R. G. *Polycyclic Aromatic Hydrocarbons*; Wiley-VCH: New York, 1997. (b) *Topics in Current Chemistry*; de Meijere, A., Ed.; Springer: Berlin, 1998; Vol. 196, Carbon Rich Compounds I. (c) *Topics in Current Chemistry*; de Meijere, A., Ed.; Springer: Berlin, 1999; Vol. 201, Carbon Rich Compounds II: Macrocyclic Oligoacetylenes and Other Linearly Conjugated Systems.

DOI: 10.1021/jo102141w Published on Web 12/23/2010

hydrocarbon peropyrene (**I**) have been replaced by nitrogen atoms (**III**).

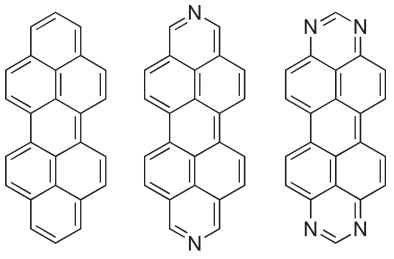

I **II** **III**

Peropyrene (**I**) itself is a highly efficient fluorophore with a quantum yield that approaches unity when dissolved in benzene and was first synthesized by Clar in 1943, by reductive coupling of two molecules of perinaphthenone.[5] Its electronic structure and photophysics have been studied extensively in recent years.[6] In contrast to the latter, diazapyrene (**II**) has been known much longer. It was first described in the literature in a German patent in 1913, and its derivatives have found applications as functional dyes.[7] The dimethyldiazaperopyrenium dicationic derivative interacts strongly with nucleotides, nucleosides, and single-stranded nucleic acids and effects their photocleavage.[8] Notably, it was also found to have nucleotide base-dependent emission behavior, and Stang et al. reported the use of diazaperopyrene as a difunctional molecular spacer in the construction of polynuclear molecular squares by connecting square planar Pd^{II} or Pt^{II} complex fragments.[9] In these applications, the low solubility of the dye molecules limits the practability of their use as molecular building blocks.[10]

Recently, we developed an efficient metal-induced synthesis of 4,9-diamino-3,10-perylenequinone diimine (**DPDI**) by oxidative coupling of two 1,8-diaminonaphthalene units[11] and demonstrated their almost quantitative conversion to derivatives of tetraazaperopyrene (**TAPP**),[12] which are potentially interesting materials for the application in organic electronic devices, in particular as n-channel semiconductors.

The low solubility of the parent compound precluded the investigation of its photophysical properties and reactivity in solution, which is why it has been extensively studied on metal surfaces to date.[13] Apart from their potential use as organic semiconducting materials, appropriately substituted tetraazaperopyrenes may act as functional dyes, since they display a rich photo and redox chemistry. In this work, we report the synthesis and characterization of new 2,9-bisaryl-substituted tetraazaperopyrene derivatives. Electron-withdrawing groups, such as F, Cl, Br, and CF_3, were introduced into the periphery of the aryl substituents. By changing the position and the number of the substituents, we were able to study the relationship between the substitution pattern in the periphery of the aryl substitutent and the photophysical and redox-chemical properties of the compounds. The nonhalogenated 2,9-bis-phenyl-1,3,8,10-tetraazaperopyrene and the alkyl substituted 2,9-bis(2,4,6-trimethylphenyl)-1,3,8,10-tetraazaperopyrene were included for comparison.

Results and Discussion

The synthesis of 2,9-bisaryl-1,3,8,10-tetraazaperopyrene (**1**−**7**) was achieved by reacting **DPDI** with a large excess of the corresponding benzoyl chloride in refluxing nitrobenzene (Scheme 1). Purification was accomplished either by sublimation at 440 °C in a weak stream of nitrogen (**1**−**3**, **6a**, **7**) or by recrystallization from nitrobenzene (**6b**−**e**). The purity of the compounds was determined by elemental analysis, and their structures were established by NMR spectroscopy.

Derivatives **1**−**7** represented in Scheme 1 may be divided into three different groups: phenyl substituted (**1**), alkylphenyl substituted (**2**), and halogenated aryl substituted

(2) For recent reviews, see: (a) Wu, J.; Pisula, W.; Müllen, K. *Chem. Rev.* **2007**, *107*, 718–747. (b) Coropceanu, V.; Cornil, J.; da Silva Filho, D. A.; Olivier, Y.; Silbey, R.; Brédas, J.-L. *Chem. Rev.* **2007**, *107*, 926–952. (c) Shirota, Y.; Kageyama, H. *Chem. Rev.* **2007**, *107*, 953–1010. (d) Katz, H. E.; Huang, J. *Annu. Rev. Mater. Res.* **2009**, *39*, 71–92. (e) Pisula, W.; Mishra, A. K.; Li, J.; Baumgarten, M.; Müllen, K. *Org. Photovoltaics* **2008**, 93–128. (f) Anthony, J. E. *Angew. Chem.* **2008**, *120*, 460–492; *Angew. Chem., Int. Ed.* **2008**, *47*, 58−77.

(3) (a) Bosdet, M. J. D.; Piers, W. E.; Sorensen, T. S.; Parvez, M. *Angew. Chem.* **2007**, *119*, 5028–5031; *Angew. Chem., Int. Ed.* **2007**, *46*, 4940−4943. (b) Takase, M.; Enkelmann, V.; Sebastiani, D.; Baumgarten, M.; Müllen, K. *Angew. Chem.* **2007**, *119*, 5620–5623; *Angew. Chem., Int. Ed.* **2007**, *46*, 5524−5527. (c) Alibert-Fouet, S.; Seguy, I.; Bobo, J.-F.; Destruel, P.; Bock, H. *Chem.—Eur. J.* **2007**, *13*, 1746–1753. (d) Qian, H.; Liu, C.; Wang, Z.; Zhu, D. *Chem. Commun.* **2006**, *44*, 4587–4589. (e) Qian, H.; Negri, F.; Wang, C.; Wang, Z. *J. Am. Chem. Soc.* **2008**, *130*, 17970–17976.

(4) (a) Chen, H. Z.; Ling, M. M.; Mo, X.; Shi, M. M.; Wang, M.; Bao, Z. *Chem. Mater.* **2007**, *19*, 816–824. (b) Schmidt, R.; Oh, J. H.; Sun, Y.-S.; Deppisch, M.; Krause, A.-M.; Radacki, K.; Braunschweig, H.; Könemann, M.; Erk, P.; Bao, Z.; Würthner, F. *J. Am. Chem. Soc.* **2009**, *131*, 6215–6228. (c) Qian, H.; Yue, W.; Zhen, Y.; Di Motta, S.; Di Donato, E.; Negri, F.; Qu, J.; Xu, W.; Zhu, D.; Wang, Z. *J. Org. Chem.* **2009**, *74*, 6275–6282.

(5) Clar, E. *Ber. Dtsch. Chem. Ges.* **1943**, *76*, 458–466.

(6) (a) Wenzel, U.; Löhmannsröben, H.-G. *J. Photochem. Photobiol. A* **1996**, 13–18. (b) Boschi, R.; Clar, E.; Schmidt, W. *J. Chem. Phys.* **1974**, *60*, 4406–4418. (c) Zander, M.; Breymann, U.; Dreeskamp, H.; Koch, E. *Z. Naturforsch. A* **1977**, *32*, 1561–1563. (d) Bergmann, I. *Trans. Faraday Soc.* **1954**, *50*, 829–838. (e) Dreeskamp, H.; Koch, E.; Zander, M. *Z. Naturforsch. A* **1975**, *30*, 1311–1314. (f) Breymann, U.; Dreeskamp, H.; Koch, E.; Zander, M. *Chem. Phys. Lett.* **1978**, *59*, 68–70. (g) Kamura, Y.; Inokuchi, H.; Aoki, J.; Fujisawa, D. *Chem. Phys. Lett.* **1977**, *46*, 356–359. (h) Miyashita, Y.; Okuyama, T.; Yamaura, K.; Jinno, K.; Sasaki, S. I. *Anal. Chim. Acta* **1987**, *202*, 237–240. (i) Agranat, I.; Suissa, M. R. *Polycyclic Aromat. Compd.* **1992**, *3*, 51–61.

(7) Kardos, M. German Patent 276357, 1913.

(8) Slama-Schwok, A.; Jazwinski, J.; Béré, A.; Montenay-Garestier, T.; Rougée, M.; Hélène, C.; Lehn, J.-M. *Biochemistry* **1989**, *28*, 3227–3234.

(9) Stang, P. J.; Cao, D. H.; Saito, S.; Arif, A. M. *J. Am. Chem. Soc.* **1995**, *117*, 6273–6283.

(10) This particular limitation has been overcome by Würthner and coworkers by way of introducing substituents in the bay position of the central perylenic core and thus permitting a systematic study of their supramolecular complexes with Pd^{II} and Pt^{II} in solution: (a) Würthner, F.; Sautter, A.; Thalacker, C. *Angew. Chem.* **2000**, *112*, 1298–1301; *Angew. Chem., Int. Ed.* **2000**, *39*, 1243−1245. (b) Sautter, A.; Schmid, D. G.; Jung, G.; Würthner, F. *J. Am. Chem. Soc.* **2001**, *123*, 5424–5430. (c) Sautter, A.; Thalacker, C.; Würthner, F. *Angew. Chem.* **2001**, *113*, 4557–4560; *Angew. Chem., Int. Ed.* **2001**, *40*, 4425−4428. (d) Würthner, F.; Sautter, A.; Schilling, J. *J. Org. Chem.* **2002**, *67*, 3037–3044. (e) Würthner, F.; Stepanenko, V.; Sautter, A. *Angew. Chem.* **2006**, *118*, 1973–1976; *Angew. Chem., Int. Ed.* **2006**, *45*, 1939−1942.

(11) (a) Hellmann, K. W.; Galka, C. H.; Rüdenauer, I.; Gade, L. H.; Scowen, I. J.; McPartlin, M. *Angew. Chem.* **1998**, *110*, 2053–2057; *Angew. Chem., Int. Ed.* **1998**, *37*, 1948−1952. (b) Gade, L. H.; Galka, C. H.; Hellmann, K. W.; Williams, R. M.; De Cola, L.; Scowen, I. J.; McPartlin, M. *Chem.—Eur. J.* **2002**, *8*, 3732–3746. (c) Gade, L. H.; Galka, C. H.; Williams, R. M.; De Cola, L.; McPartlin, M.; Dong, B.; Chi, L. *Angew. Chem.* **2003**, *115*, 2781–2785; *Angew. Chem., Int. Ed.* **2003**, *42*, 2677−2681. (d) Stöhr, M.; Wahl, M.; Galka, C. H.; Riehm, T.; Jung, T. A.; Gade, L. H. *Angew. Chem.* **2005**, *117*, 7560–7564; *Angew. Chem., Int. Ed.* **2005**, *44*, 7394−7398. (e) Wahl, M.; Stöhr, M.; Spillmann, H.; Jung, T. A.; Gade, L. H. *Chem. Commun.* **2007**, 1349–1351. (f) Lobo-Checa, J.; Matena, M.; Müller, K.; Dil, J. H.; Meier, F.; Gade, L. H.; Jung, T. A.; Stöhr, M. *Science* **2009**, *325*, 300–303.

(12) Riehm, T.; De Paoli, G.; Konradsson, A. E.; De Cola, L.; Wadepohl, H.; Gade, L. H. *Chem.—Eur. J.* **2007**, *13*, 7317–7329.

(13) (a) Matena, M.; Riehm, T.; Stöhr, M.; Jung, T. A.; Gade, L. H. *Angew. Chem.* **2008**, *120*, 2448–2451; *Angew. Chem., Int. Ed.* **2008**, *47*, 2414−2417. (b) Matena, M.; Stöhr, M.; Riehm, T.; Björk, J.; Martens, S.; Dyer, M. S.; Persson, M.; Lobo-Checa, J.; Müller, K.; Enache, M.; Wadepohl, H.; Zegenhagen, J.; Jung, T. A.; Gade, L. H. *Chem.—Eur. J.* **2010**, *16*, 2079–2091.

SCHEME 1. Synthesis of 2,9-Bisaryl-1,3,8,10-tetraazaperopyrene Derivatives

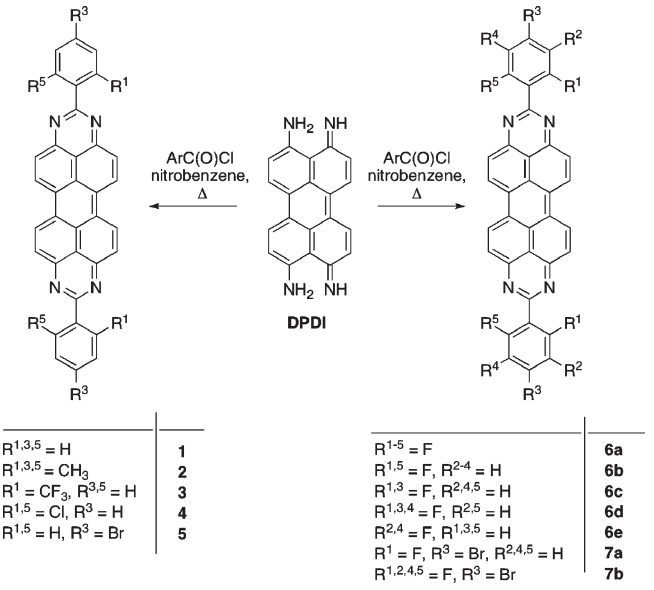

tetraazaperopyrenes (**3**−**7**). The examination of the properties of these compounds was limited by their low solubility in common organic solvents. The substitution in *ortho* position of the phenyl group usually led to an increase in solubility. Among all derivatives only *ortho*-substituted phenyl congeners were sufficiently soluble for studying solutions of defined concentration in organic solvents. This effect is probably due to the twist of the aryl substituent, which is imposed by steric repulsion between the *ortho* substituents and the peropyrene core and impedes efficient aromatic stacking upon crystallization (vide infra). A similar behavior has already been observed by Langhals for *o*-phenyl substituted 3,4,9,10-perylene bisimides.[14]

Given the lack of solubility in organic solvents, NMR spectra were recorded either in deuterated trifluoroacetic acid or concentrated deuterated sulfuric acid, in which they readily dissolved without decomposition. Irrespective of the substituents in position 2 and 9, the resonances observed in the ^{13}C NMR spectra are almost identical for the central polycondensed arene moiety. In the ^{1}H NMR spectra CH proton resonances of the peropyrene core were detected between 10.44 and 10.76 ppm (H^a) and 9.21 and 9.41 ppm (H^b) with coupling constants ranging from 9.3 to 9.7 Hz for all compounds.

Crystal Structures. Crystals suitable for X-ray diffraction of compounds **3**, **6a**, **6b**, and **7b** were grown by sublimation at 440 °C in a horizontal glass tube in a weak stream of nitrogen. All solid state structures show crystallographic C_i molecular symmetry without exception. Their molecular structures are determined by the planar tetraazaperopyrene core with almost identical bond lengths and angles and the phenyl substituents rotated out of the plane of the polycyclic molecular core to reduce the steric repulsion. As an example, the top and side views of **6a** are depicted in Figure 1.

As expected, the interplanar angles show a dependence on the size of the *ortho* substituent (see Table 1). Interesting to note is the difference of the interplanar angle in the crystal structures of **6a**, **6b**, and **7b**, which all contain fluorine atoms in both *ortho* positions of the phenyl substituent on the one hand and the deviation of the interplanar angles in the two independent molecules of the solid state structures of **3** and **6b** (**3**, 73.83° vs 86.13°; **6b**, 65.87° vs 57.25°) on the other hand. These observations can be taken as an indication for a shallow potential energy minimum for the rotational orientation of the aryl substituents.

The intermolecular packing pattern of all compounds is characterized by parallel stacks of molecules. The interplanar distances between the aromatic cores of neighboring molecules within a column lie in the range of about 3.4 Å for all structures. This value is close to the $\pi-\pi$ stacking distance of 3.37 Å found in graphite,[16] and is also in good accordance with the range of 3.34−3.55 Å previously established for perylene bisimides.[17]

The relative orientation of the individual molecules within the stacks is governed by the steric requirements of the substituted phenyl rings. Neighboring molecules of **3**, for instance, are rotated by 43° within the molecular plane with respect to one another (Figure 2), while they are superposed in the case of **6a**. The differences in the packing efficiency are also obvious from the Kitajgorodskij packing index[15] (percentage of filled space, Table 1).

The views of molecular stacking chosen in Figure 2 illustrate how the larger interplanar angle of the phenyl ring bearing a trifluoromethyl group in the *ortho* position leads to the increased $\pi-\pi$ stacking distance (**3**, 3.46 Å vs **6b**, 3.36 Å) as well as to the above-mentioned relative orientation of the molecules within the stack. In both cases (**3** and **6b**) weak intermolecular hydrogen bonds are found between the fluorine atoms of the phenyl groups and the *ortho* hydrogen atoms of the peropyrene core of the neighboring molecules (**3**, 2.49 Å, **6b**, 2.52−2.57 Å).

A different situation is observed for the solid state structures of **6a** and **7b**. In both crystal structures the molecules are superposed within the stacks and the long axes of the molecules in neighboring stacks are not parallel orientated but tilted along the molecule axes relative to each other (herringbone arrangement, Figure 3). This closely resembles the situation found for the X-ray analyses of the recently published 2,9-bis(2-bromophenyl)-1,3,8,10-tetraazaperopyrene.[12]

To date, all crystallographically characterized **TAPP** derivatives were crystallized either by sublimation in a stream of nitrogen (**3**, **6a**, **6b**, **7b**) or from an organic solvent (2,9-bis(2-bromophenyl)-1,3,8,10-tetraazaperopyrene). However, in this study we were able to grow crystals of a **TAPP** derivative suitable for X-ray diffraction from trifluoroacetic acid (TFA) for the first time, thus allowing a closer examination of the protonation pattern pertinent to the photophysical studies in acids (vide infra). The solid state structure reveals a 2-fold protonated species, which directly indicates the previously proposed degree of protonation in this acidic solvent as shown by titration for alkyl substituted **TAPP**s.[12]

(14) (a) Rademacher, A.; Märkle, S.; Langhals, H. *Chem. Ber.* **1982**, *115*, 2927–2934. (b) Langhals, H.; Demming, S.; Huber, H. *Spectrochim. Acta* **1988**, *44A*, 1189–1193.

(15) Kitajgorodskij, A. I. *Molecular Crystals and Molecules*; Head Press: New York, 1973.

(16) Forrest, S. R.; Kaplan, M. L.; Schmidt, P. H. *J. Appl. Phys.* **1984**, *55*, 1492–1507.

(17) Klebe, G.; Graser, F.; Hädicke, E.; Berndt, J. *Acta Crystallogr., Sect. B* **1989**, *45*, 69–77.

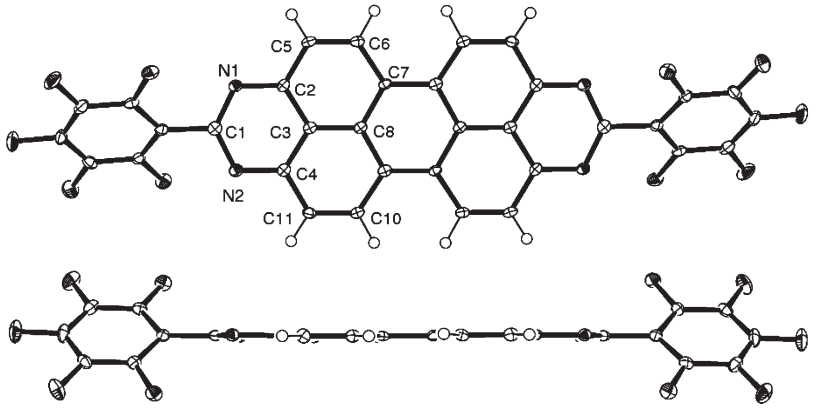

FIGURE 1. Molecular structure of **6a**: top view (top) and side view (bottom). Thermal ellipsoids were drawn at the 50% probability level.

TABLE 1. Selected Details of Crystal Structures of Compounds 3, 6a, 6b, and 7b

	3	6a	6b	7b
crystal system	monoclinic	monoclinic	triclinic	monoclinic
$\pi-\pi$ plane distance	3.46 Å	3.37 Å	3.36 Å	3.36 Å
interplanar angle (expt)[a]	73.82°/86.13°	41.10°	65.87°/57.25°	43.51°
interplanar angle (DFT)[b]	38.67°	47.74°	48.98°	48.34°
packing index[c]	70.6%	75.7%	72.5%	72.3%

[a]Interplanar angle between the peropyrene core and the phenyl substituent; in the case of compound **3** and **6b** two independent molecules with unequal interplanar angles were observed in the single crystal. [b]Calculated at the B3PW91/6-31g(d,p) level of theory. [c]Determined according to literature methods.[15]

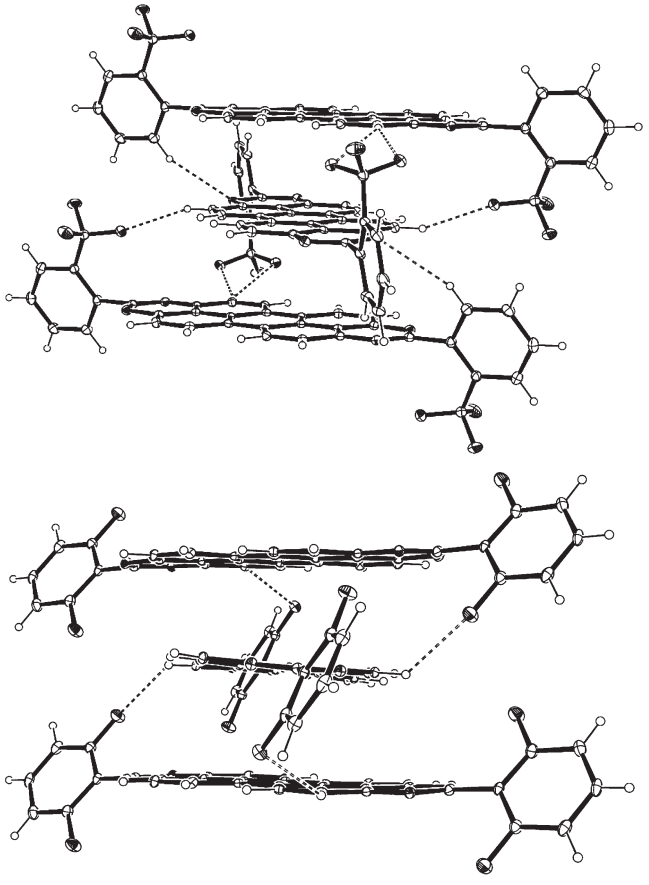

FIGURE 2. Crystal packing of **3** (top) and **6b** (bottom) in the crystal form showing the twisted arrangement of the aryl substituents and weak hydrogen interactions. Thermal ellipsoids were drawn at the 30% probability level.

Although twinning of the crystals, severe disorder within the trifluoromethyl groups, and an apparent rotational disorder (presumably due to dynamic effects) of the pentafluorophenyl groups, which could not be modeled accurately with a split-atom model, restrained the structure determination, it was still possible to determine the 2-fold protonation of the tetraazaperopyrene. Inspection of the internal geometry of the potential trifluoroacetic acid and/or trifluoroacetate moieties revealed the presence of two trifluoroacetate and six trifluoroacetic acid molecules per molecule of H_2**6a**$^{2+}$. On the basis of the short contact distance of 2.80 Å between N(1) and the oxygen of a trifluoroacetic acid molecule (Figure 4), which lies in the range of a N−H···O hydrogen bond, N(1) was identified as the protonation site N(1). The position of H(1) was indeed found from a difference Fourier synthesis and could be refined satisfactorily.

The protonated molecules are arranged in parallel stacks along the shorter cell axis with an intermolecular stacking distance of 7.93 Å and having solvent molecules placed between the layers. On the basis of the repulsive coulomb interaction between the (charged) protonated molecules, the dramatically increased stacking distance as well as the incorporated solvent molecules, the presence of $\pi-\pi$ interaction can no longer be assumed for this species.

Notably, no significant change of bond lengths and angles of the tetraazaperopyrene core is observed comparing the X-ray analyses of the unprotonated and protonated species. Only the torsion angle of the phenyl substituent is clearly increased (**6a**, 40.2° vs H_2**6a**$^{2+}$, 47.0°).

Theoretical Modeling of the Structures and Frontier Orbital Levels. The ground-state geometries of the **TAPP** derivatives were calculated at the B3PW91/6-31g(d,p) level of DFT, followed by frequency analyses to verify the energy minima. In general, the optimized structures were in good agreement

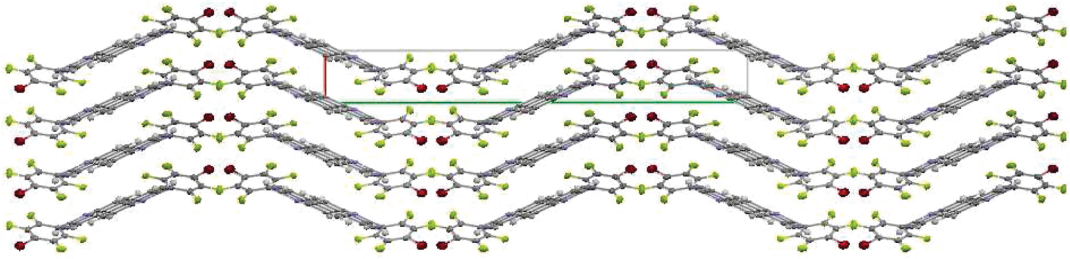

FIGURE 3. Herringbone arrangement of the molecules of **7b** in the crystal form.

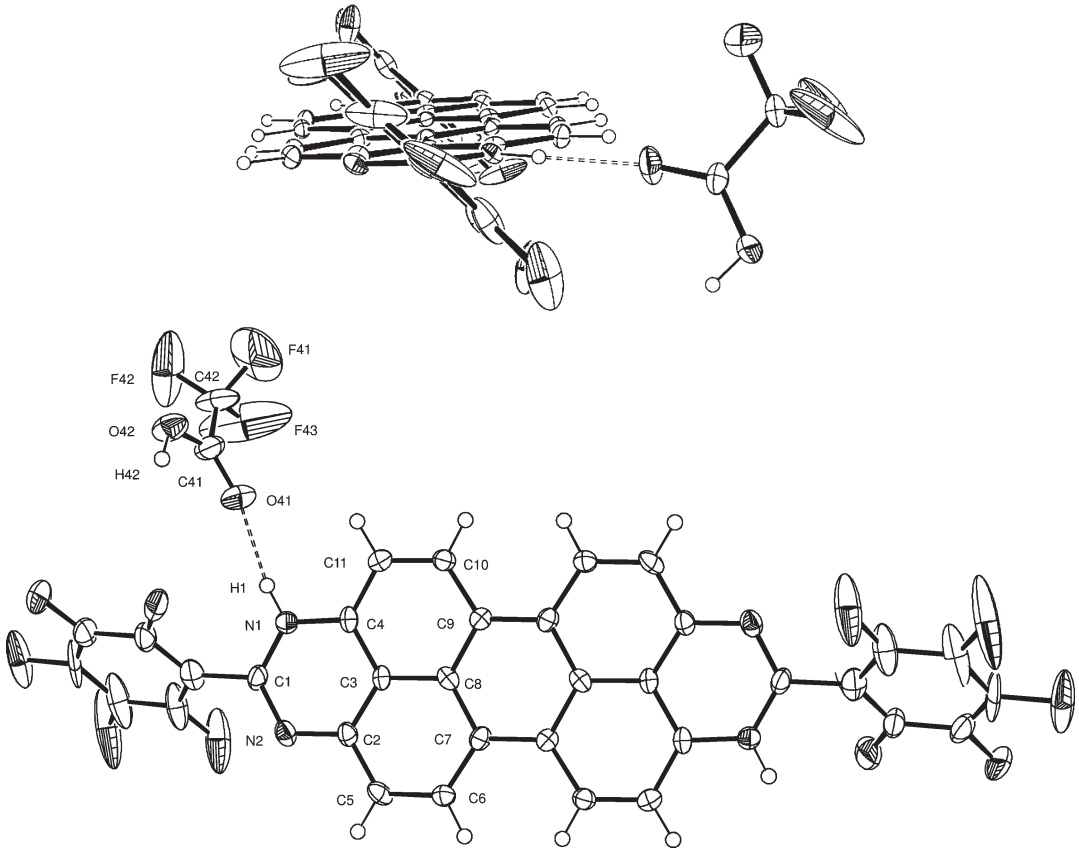

FIGURE 4. Molecular structure of H_2**6a**$^{2+}$. Front view (top) and top view (bottom). Thermal ellipsoids were drawn at the 30% probability level. Trifluoroacetate anion and all except one trifluoroacetic acid molecules have been omitted for clarity.

with the metric parameters of the crystallographically characterized tetraazaperopyrene derivatives. Only the interplanar angle of the aryl substituent deviated considerably (Table 1), which is probably due to the fact that the calculations were performed on single molecules in the gas phase.

Nevertheless for compounds **6a**, **6b**, and **7b** the computational studies reflect the qualitative trend of the interplanar angle, while it is not surprising that the experimental value of the interplanar angle of compound **3** is significantly different for the DFT optimized and the crystal structure (X-ray, 71.4° vs DFT, 37.4°). Since the trifluoromethyl group is significantly larger than a single fluorine atom, it will give rise to the strongest steric hindrance, and therefore the intermolecular interactions in the solid state are expected to be more relevant than for the fluorine substituted derivatives as is also illustrated in Figure 2.

According to the calculations, the frontier molecular orbital energies depend on the substitution pattern, despite the fact that because of the symmetry of the core system all frontier molecular orbitals have a nodal plane at the long axis of the molecules, running through the substituted carbon atoms. The calculated gas-phase lowest unoccupied molecular orbital (LUMO) energies for the soluble derivatives are summarized in Table 2. According to these calculations, a trend on going from an alkyl-substituted aryl to a fluorophenyl substituent is observed. The insertion of an electron-withdrawing group leads to the expected decrease in LUMO energy. In addition to that, the computed electron affinities (EA) exhibit the same trend. EAs were determined by optimizing the structure of the anionic species, using the previously optimized geometry of the neutral species as a starting point and taking the difference of the total energies of both species (see Supporting Information for the full set of Kohn−Sham frontier molecular orbital energies and total energies for all derivatives discussed in this work).

TABLE 2. Cyclovoltammetric Data for Soluble Compounds

compound	E_{red1} [V][a]	E_{red2} [V]	E_{LUMO} [eV][b]	E_{LUMO} [eV][c]	EA [eV][c]
2	−0.89	−1.17	−3.44	−3.13	2.06
3	−0.86	−1.14	−3.50	−3.23	2.15
6a	−0.74	−1.01	−3.61	−3.47	2.37
6b	−0.81	−1.09	−3.55	−3.17	2.06

[a]Measured against SCE in CH_2Cl_2. [b]Determined according to literature methods,[18] using Fc/Fc^+ as an internal standard. [c]Calculated at the B3PW91/6-31g(d,p) level of theory.

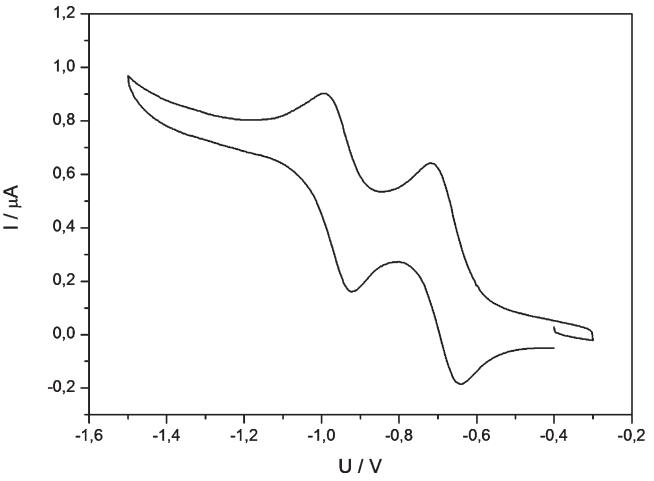

FIGURE 5. Cyclic voltammogram of **6a** recorded in CH_2Cl_2 (sweep rate 50 mV s^{-1}; supporting electrolyte Bu_4NPF_6).

To put these results of our theoretical modeling to an experimental test, we employed cyclic voltammetry to evaluate the substituent effects on the highest occupied molecular orbital (HOMO) and the LUMO of the peropyrene core. The cyclic voltammograms of the soluble derivatives (**2**, **3**, **6a**, **6b**) displayed two reversible one-electron reduction waves that correspond to the sequential formation of the mono- and dianionic species. The electrochemical data are summarized in Table 2.

The cyclic voltammogram of **6a** (Figure 5) displays two reversible redox waves with half wave potentials at $E_{red1} = -0.74$ V and $E_{red2} = -1.01$ V (vs SCE) with a difference between the cathodic and anodic wave of about 70 mV in each case. The observation of an i_a/i_c ratio of exactly 1 and a relationship of $i_p \approx \nu^{1/2}$ indicate the reversibility of the electrochemical process. Recording the CV in the presence of ferrocene as an internal standard established them to be two one-electron reductions and in addition to that allowed the estimation of the LUMO energy levels.[18]

The comparison of the experimental values reveals a decrease of the LUMO energies of the derivatives bearing a fluorophenyl substituent (**2**, −3.44 eV vs **6a**, −3.61 eV). This observation confirms the assumption that by insertion of electron-withdrawing groups such as fluoro substituted phenyl a stabilization of the mono- and dianionic species is achieved. By increasing the number of the highly electronegative fluorine substituents on the phenyl group, the electron-withdrawing capability of the phenyl substituent and therefore the stabilization of the mono- and dianionic species is enhanced. A similar situation was observed by Chen and Bao et al.[4a] and Würthner et al.[4b] for perylenebisimides.

UV−vis Absorption Spectra and Emission Behavior. All of the tetraazaperopyrene derivatives **1**−**7** reported in this work

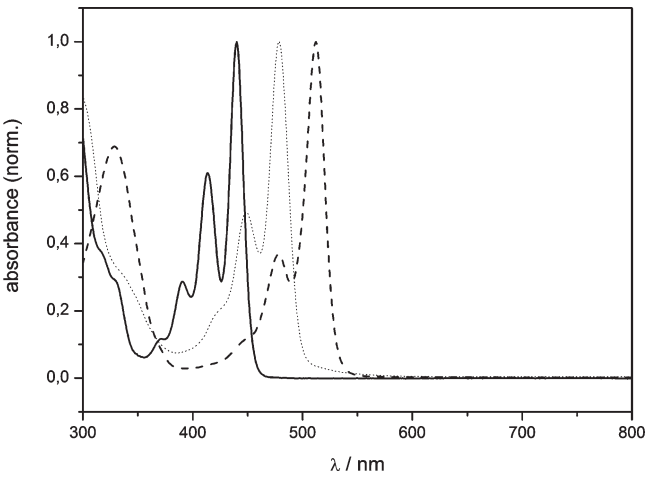

FIGURE 6. Normalized UV−vis absorption spectra of compound **6a** measured in diluted solutions (10^{-5} mol/L) in toluene (solid line), TFA (dotted line), and concentrated sulfuric acid (dashed line).

TABLE 3. $\pi^*\leftarrow\pi$ Transition λ_{max} [nm] and Vibrational Progression $\Delta\nu$ [cm^{-1}] in the Absorption Spectra Recorded in TFA

compound	λ_{max} (log ε) [nm], $\Delta\nu$ [cm^{-1}]	λ_{em} (Stokes shift) [nm]	ϕ
1	479 (4.94), 1395	519 (40)	0.03
2	478 (4.81), 1209	491 (13)	< 0.01
3	478 (4.90), 1401	490 (12)	0.30
4	478 (4.89), 1401	490 (12)	0.02
5	483 (4.80), 1420	529 (46)	< 0.01
6a	478 (4.97), 1401	491 (13)	0.29
6b	479 (5.01), 1395	496 (17)	0.06
6c	479 (4.64), 1445	511 (32)	0.17
6d	480 (4.90), 1438	507 (27)	0.16
6e	480 (4.93), 1438	504 (24)	0.15
7a	481 (4.89), 1432	520 (39)	< 0.01
7b	479 (5.04), 1395	520 (41)	0.05

are yellow to brown in the solid state and yellow to orange in solution, depending on the concentration. Because of their lack of solubility in common organic solvents, a systematic study of the optical properties for all derivatives was conducted in trifluoroacetic acid (TFA). The UV−vis absorption spectra of compounds **1**−**7** recorded in neat TFA are almost superimposable. They display a characteristic visible absorption band between 460 and 490 nm (log $\varepsilon = 4.64-5.01$, Table 3). The band is characterized by a strong vibrational progression of about 1173−1475 cm^{-1} as it is typical for $\pi^*\leftarrow\pi$ transition in polycondensed aromatics and in particular for perylene derivatives.[19] The absence of, basically, any effect of the substituents in position 2 and 9 on the absorption spectra indicates that their influence on the HOMO−LUMO gap of the tetraazaperopyrene core is negligible, as we already observed previously for the alkyl substituted derivatives.[12] As noted above, this is due to the fact that a nodal plane in the

(18) Seguy, I.; Jolinat, P.; Destruel, P.; Mamy, R.; Allouchi, H.; Courseille, C.; Cotrait, M.; Bock, H. *ChemPhysChem* **2001**, *7*, 448–452.

(19) (a) Feiler, L.; Langhals, H.; Polborn, K. *Liebigs Ann.* **1995**, 1229–1244. (b) Langhals, H. *Helv. Chim. Acta* **2005**, *88*, 1309–1343. (c) Sadrai, M.; Bird, G. R. *Opt. Commun.* **1984**, *51*, 62–64. (d) Löhmannsröben, H. G.; Langhals, H. *Appl. Phys. B: Laser Opt.* **1989**, *48*, 449–452. (e) Ford, W. E.; Kamat, P. V. *J. Phys. Chem.* **1987**, *91*, 6373–6380. (f) Rohr, U.; Schlichting, P.; Böhm, A.; Gross, M.; Meerholz, K.; Bräuchle, C.; Müllen, K. *Angew. Chem.* **1998**, *110*, 1463–1467; *Angew. Chem., Int. Ed.* **1998**, *37*, 1434−1437. (g) Langhals, H.; Karolin, J.; Johannson, L. B. A. *J. Chem. Soc., Faraday Trans.* **1998**, *94*, 2919–2922.

TABLE 4. LUMO Energies of Fluorine Substituted TAPP Derivates and Compounds 1 and 2 as References, Calculated at the B3PW91/6-31g(d,p) Level of Theory, Listed in Order of Their Energy Level

	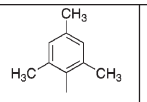								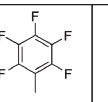	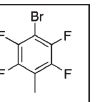
	2	**1**	**6b**	**6c**	**3**	**7a**	**6d**	**6e**	**6a**	**7b**
LUMO-energy [eV][a]	-3.13	-3.14	-3.17	-3.22	-3.23	-3.29	-3.32	-3.38	-3.47	-3.49
Φ	<0.01	0.03	0.06	0.17	0.30	<0.01	0.16	0.15	0.29	0.05

[a]Calculated at the B3PW91/6-31g(d,p) level of theory.

HOMO and LUMO is present running through the carbon atoms 2 and 9. Exemplary studies in toluene, trifluoroacetic acid, and sulfuric acid have been carried out with compound **6a** to verify the protonation steps (Figure 6).[12]

On going from an organic solvent to TFA the protonation of two nitrogen atoms occurs, whereas the protonation of all four nitrogen atoms is achieved in an even more acidic medium such as concentrated sulfuric acid.

The fluorescence spectra of compounds **1**−**7** recorded in TFA are characterized by an emission band between 490 and 530 nm with the characteristic vibrational progression (Table 3). The emission spectra display the mirror symmetry of the absorbance spectra with Stokes shifts of 10−50 nm. The luminescence quantum yields range from < 0.01 to 0.30, thereby indicating a quenching effect for some substitution patterns.

In an early study, Langhals et al. found that the quantum yields observed for different phenyl substituted perylenebisimides are dependent on the steric hindrance in *ortho* position, since the rotation of the phenyl substituents is a favored pathway for the radiationless deactivation of excited molecules.[14] For our systems, we observed that the electronic structure of the molecules **1**−**7** had a significant influence on the quantum yields. Most recently, Flamingi and Langhals et al. reported on a similar effect, focusing on the mechanism of luminescence quenching by different electron-rich substituents.[20]

The enhancement of solubility by forcing an expanded polycyclic aromatic system in a twisted conformation and thereby inhibiting the molecular stacking is an effect reported by Würthner et al. for their core substituted perylenbisimides.[21] As it turns out, for the **TAPP** derivatives a sterically more demanding *ortho* substituent does not automatically lead to a greater increase of solubility. While the insertion of a fluorine atom, an alkyl group or a perfluorinated alkyl group induced a significant enhancement of solubility in comparison to the unsubstituted 2,9-bis-phenyl-1,3,8,10-tetraazaperopyrene, only a slight improvement was observed for derivatives bearing a chlorine or bromine atom in *ortho* position. More importantly, heavy atoms such as chlorine and bromine seem to cause fluorescence quenching, which is a known but as yet incompletely understood phenomenon.[22]

The highest quantum yields of around 30% were found for the perfluorophenyl substituted **TAPP** derivative **6a** and the 2-trifluoromethyl phenyl substituted derivative **3**. Interestingly, the location of the fluorine substituents on the phenyl group seems to be of importance. Whereas derivates **6b** and **7b**, in particular, with the same sterical hindrance regarding the phenyl rotation, exhibited an emission quantum yield of 5−6%, the emission of compounds **6c**−**e** occurred with quantum yields of up to 17%, indicating a positive effect of the fluorine atoms in the *meta* and *para* positions of the phenyl ring. This observation is further supported by the comparison of **5**, **7a**, and **7b**. Whereas the fluorescence of **5** and **7a** appeared to be quenched ($\Phi = < 1\%$) probably as a result of the bromine sustituent, derivative **7b** exhibited an emission quantum yield of approximately 5%. The same effect is observed comparing **6b** (Φ = 6%) with **6c**−**e** (Φ = 15−17%).

The theoretical modeling of the energy levels (Table 4) also indicated a special effect of the *ortho* and *para* substituents, since the LUMO energies of **TAPP** derivatives bearing fluorine substituents in the *meta* or *para* position are lowered, with the effect of the *meta* substituent being stronger. In Table 4 the fluorine substituted **TAPP** derivatives (and compound **1** and **2** for comparison) are listed in order of decreasing LUMO energy level. The fluorescence quantum yields of the **TAPP** derivatives increased with decreasing LUMO energy, with the exception of **7a** and **7b**, which both contain a bromo substituent (see discussion above), and compound **3**. For the latter neither the optimized structure nor the calculated LUMO energies are in good accordance with the experimental data. As already discussed above, this is probably due to intermolecular interactions that we were not able to model adequately with our methods.

Therefore, we assume that in the case of **3**, the higher emission quantum yield is more specifically related to steric effects that result in a significant improvement of solubility

(20) Flamigni, L.; Ventura, B.; Barbieri, A.; Langhals, H.; Wetzel, F.; Fuchs, K.; Walter, A. *Chem.—Eur. J.* **2010**, *16*, 13406–13416.

(21) See for example: (a) Gsänger, M.; Hak, Oh, J.; Könemann, M.; Höffken, H. W.; Krause, A.-M.; Bao, Z.; Würthner, F. *Angew. Chem.* **2010**, *122*, 752–755; *Angew. Chem., Int. Ed.* **2010**, *49*, 740−743. (b) Würthner, F. *Chem. Commun.* **2004**, 1564–1579. (c) Chen, S.; Debije, M. G.; Debaerdemaeker, T.; Osswald, P.; Würthner, F. *ChemPhysChem* **2004**, *5*, 137–140.

(22) (a) Lakowicz, J. R. *Principles of Fluorescence Spectroscopy*, 3rd ed.; Springer: New York, 2006. (b) Martinho, J. M. C. *J. Phys. Chem.* **1989**, *93*, 6687–6692.

and inhibition of aggregation rather than being due to the electronic properties induced by the substituents.

Conclusions

In this work we have presented the synthesis and characterization of a selection of aryl substituted tetraazaperopyrene dyes. By growing crystals of a **TAPP** derivative suitable for X-ray diffraction from TFA, we were able to prove the previously postulated 2-fold protonation of the tetraazaperopyrene derivatives in this acidic solvent.

The effect of a series of electron-withdrawing substituents on the periphery of an aryl group directly connected to a tetraazaperopyrene on the electronic and optical properties has been examined. The absorption and emission spectra, almost superimposable for all compounds investigated, indicated an insignificant effect of the substituents on the HOMO−LUMO gap. In contrast to these observations, the fluorescence quantum yields range from approximately 1% to 30%, thus displaying considerable dependence on the electronic properties of the substituent. This is in accordance with the results of a theoretical modeling of their energy levels, which revealed that the insertion of electron-withdrawing groups leads to a decrease of, particularly, the LUMO energies.

The computed LUMO energies and electron affinities of the **TAPP** derivatives and the possibility to increase them further by introduction of electron-withdrawing substituents at the central aromatic core makes these materials promising candidates for the development of organic n-channel semiconductors. Such work is currently under way in our laboratory.

Experimental Section

General Procedure for the Preparation of the Tetraazaperopyrene (TAPP) Derivatives. To a suspension of 310 mg (1 mmol) of 4,9-diaminoperylene-quinone-3,10-diimine (**DPDI**)[11] in 25 mL of nitrobenzene was added 12 mmol of the corresponding acid chloride, and the mixture was heated to reflux for 6 h. The mixture was allowed to cool to room temperature. The resulting suspension was filtered and washed several times with acetone, ethanol, and finally pentane (200 mL). The brown solids were either recrystallized from nitrobenzene or purified by sublimation at 440 °C in a nitrogen stream.

2,9-Bis-phenyl-1,3,8,10-tetraazaperopyrene (1). Acid chloride: benzoyl chloride. Yield: 381 mg (0.8 mmol; 79%) of **1** as an orange powder. ^{1}H NMR (600.13 MHz, TFA-d_1) δ 10.56 (d, 4H, ^3J = 9.6 Hz, H^b), 9.33 (d, 4H, ^3J = 9.4 Hz, H^a), 8.77 (d, 4H, ^3J = 7.6 Hz, H$_{Ar}$), 8.03 (t, 2H, H$_{Ar}$), 7.95 (t, 4H, H$_{Ar}$). ^{13}C NMR (150.92 MHz, TFA-d_1, 295 K) δ 159.9 (C7), 154.3 (C6), 140.2 (C4H^b), 137.7 (C11), 132.5 (C10H$_{Ar}$), 132.0 (C8), 131.9 (C3H$_{Ar}$), 131.6 (C9H$_{Ar}$), 128.7 (C5H^a), 123.1 (C2), 116.3 (C1). HRMS (EI): m/z calcd for $C_{34}H_{18}N_4$ 482.1531, found 482.1506. Anal. Calcd for $C_{34}H_{18}N_4$: C 84.63, H 3.76, N 11.61. Found: C 84.34, H 3.72, N 11.50.

2,9-Bis(2,4,6-trimethyl-phenyl)-1,3,8,10-tetraazaperopyrene (2). Acid chloride: 2,4,6-trimethylbenzoyl chloride. Yield: 410 mg (0.7 mmol; 72%) of **2** as yellow powder. ^{1}H NMR (399.98 MHz, TFA-d_1) δ 10.58 (d, 4H, ^3J = 9.5 Hz, H^b), 9.28 (d, 4H, ^3J = 9.3 Hz, H^a), 7.17 (s, 4H, H$_{Ar}$), 2.41 (s, 6H, *para*-CH$_3$), 2.20 (s, 12H, *ortho*-CH$_3$). ^{13}C NMR (150.92 MHz, TFA-d_1, 295 K) δ 163.1 (C7), 153.6 (C6), 146.7 (C11), 141.2 (C4H^b), 139.3 (C9), 132.4 (C3), 131.6 (C10H$_{Ar}$), 128.8 (C8), 128.3 (C5H^a), 122.9 (C2), 116.4 (C1), 21.9 (*para*-CH$_3$), 20.5 (*ortho*-CH$_3$). HRMS (MALDI): m/z calcd for $C_{40}H_{31}N_4$ 567.2549, found 567.2543. Anal. Calcd for $C_{40}H_{30}N_4$: C 84.78, H 5.34, N 9.89. Found: C 84.60, H 5.70, N 9.60.

2,9-Bis(2-trifluoromethyl-phenyl)-1,3,8,10-tetraazaperopyrene (3). Acid chloride: 2-trifluoromethylbenzoyl chloride. Yield: 300 mg (0.5 mmol; 49%) of **3** as a yellow powder. ^{1}H NMR (600.13 MHz, TFA-d_1) δ 10.54 (d, 4H, ^3J = 9.5 Hz, H^b), 9.22 (d, 4H, ^3J = 9.3 Hz, H^a), 8.05 (d, 2H, ^3J = 7.9 Hz, H$_{Ar}$), 7.98−7.91 (m, 4H, H$_{Ar}$), 7.89 (t, 2H, ^3J = 7.2 Hz, H$_{Ar}$). ^{13}C NMR (150.90 MHz, TFA-d_1, 295 K) δ 159.7 (C7), 153.6 (C6), 141.1 (C4H^b), 135.5 (C11H$_{Ar}$), 134.7 (C12), 133.7 (C13), 132.4 (C3), 132.3 (quar, $^2J_{CF}$ = 32.6 Hz, C9), 131.0 (C8), 129.9 (quar, $^3J_{CF}$ = 4.8 Hz, C10H$_{Ar}$), 128.7 (C5H^a), 125.7 (quar, $^1J_{CF}$ = 274.4 Hz, CF$_3$), 122.8 (C2), 116.5 (C1). HRMS (MALDI): m/z calcd for $C_{36}H_{17}F_6N_4$ 619.1357, found 619.1352. Anal. Calcd for $C_{36}H_{16}F_6N_4$: C 69.91, H 2.61, N 9.06. Found: C 70.00, H 2.90, N 9.06.

2,9-Bis(2,6-dichloro-phenyl)-1,3,8,10-tetraazaperopyrene (4). Acid chloride: 2,6-dichlorobenzoyl chloride. Yield: 407 mg (0.7 mmol; 66%) of **4** as a brown powder. ^{1}H NMR (600.13 MHz, TFA-d_1) δ 10.76 (d, 4H, ^3J = 9.6 Hz, H^b), 9.46 (d, 4H, ^3J = 9.3 Hz, H^a), 7.81 (m, 6H, H$_{Ar}$). ^{13}C NMR (150.92 MHz, TFA-d_1, 295 K) δ 157.0 (C7), 154.0 (C6), 141.2 (C4), 137.0 (C8), 136.7 (C11), 132.6 (C3), 131.5 (C9), 131.1 (C10), 128.8 (C5), 122.9 (C2), 116.8 (C1). HRMS (FAB): m/z calcd for $C_{34}H_{15}N_4Cl_4$ 619.0051, found 619.0081.

2,9-Bis(4-bromo-phenyl)-1,3,8,10-tetraazaperopyrene (5). Acid chloride: 4-bromobenzoyl chloride. Yield: 477 mg (0.7 mmol; 57%) of **5** as a yellow powder. ^{1}H NMR (600.13 MHz, TFA-d_1) δ 10.47 (d, 4H, ^3J = 9.6 Hz, H^b), 9.23 (d, 4H, ^3J = 9.2 Hz, H^a), 8.59 (d, 4H, ^3J = 8.3 Hz, H$_{Ar}$), 8.01 (d, 4H, ^3J = 8.8 Hz, H$_{Ar}$). ^{13}C NMR (150.92 MHz, TFA-d_1, 295 K) δ 158.7 (C7), 154.2 (C6), 140.0 (C4H^b), 135.8 (C10H$_{Ar}$), 133.7 (C11), 132.5 (C9H$_{Ar}$), 131.8 (quar, C3), 130.5 (C8), 128.6 (C5), 123.0 (C2), 116.1 (C1). HRMS (EI): m/z calcd for $C_{34}H_{16}N_4Br_2$ 637.9742, found 637.9764. Anal. Calcd for $C_{34}H_{16}N_4Br_2$: C 63.77, H 2.52, N 8.75. Found: C 63.73, H 2.62, N 8.69.

2,9-Bis(2,3,4,5,6-pentafluoro-phenyl)-1,3,8,10-tetraazaperopyrene (6a). Acid chloride: 2,3,4,5,6-pentafluorobenzoyl chloride. Yield: 434 mg (0.7 mmol; 66%) of **6a** as an orange powder. ^{1}H NMR (600.13 MHz, TFA-d_1) δ 10.71 (d, 4H, ^3J = 9.4 Hz, H^b), 9.32 (d, 4H, ^3J = 9.3 Hz, H^a). ^{13}C NMR (150.92 MHz, TFA-d_1, 295 K) δ 154.2 (C7), 149.8 (C6), 148.0, 148.1 (C9/C11), 141.0 (C10), 140.9 (C4H^b), 132.5 (C3), 129.0 (C5H^a), 122.8 (C2), 116.6 (C1), 109.2 (C8). HRMS (EI): m/z calcd for $C_{34}H_8N_4F_{10}$ 662.0589, found 662.0545. Anal. Calcd for $C_{34}H_8N_4F_{10}$ (662.4): C 61.65 H 1.22 N 8.46. Found: C 61.37 H 1.35 N 8.47.

2,9-Bis(2,6-difluoro-phenyl)-1,3,8,10-tetraazaperopyrene (6b). Acid chloride: 2,6-difluorobenzoyl chloride. Yield: 400 mg (0.7 mmol; 72%) of **6b** as an orange powder. ^{1}H NMR (600.13 MHz, TFA-d_1) δ 10.58 (d, 4H, ^3J = 9.6 Hz, H^b), 9.30 (d, 4H, ^3J = 9.4 Hz, H^a), 7.85 (m, 2H, H$_{Ar}$), 7.33 (m, 4H, H$_{Ar}$). ^{13}C NMR (150.92 MHz, TFA-d_1, 295 K) δ 163.1 (dd, $^1J_{CF}$ = 257.3 Hz, $^3J_{CF}$ = 4.9 Hz, C9), 153.9 (C6), 152.5 (C7), 140.8 (C4H^b), 139.1 (t, $^3J_{CF}$ = 10.7 Hz, C11H$_{Ar}$), 132.4 (C3), 128.7 (C5H^a), 122.8 (C2), 116.4 (C1), 115.1 (dd, $^2J_{CF}$ = 21.1 Hz, $^4J_{CF}$ = 3.4 Hz C10H$_{Ar}$), 111.1 (t, $^2J_{CF}$ = 15.9 Hz, C8). HRMS (FAB): m/z calcd for $C_{34}H_{15}N_4F_4$ 555.1233, found 555.1230. Anal. Calcd for $C_{34}H_{14}N_4F_4$: C 73.65, H 2.54, N 10.10. Found: C 73.77, H 2.62, N 10.13.

2,9-Bis(2,4-difluoro-phenyl)-1,3,8,10-tetraazaperopyrene (6c). Acid chloride: 2,4-difluorobenzoyl chloride. Yield: 410 mg (0.7 mmol; 74%) of **6c** as an orange powder. ^{1}H NMR (600.13 MHz, TFA-d_1) δ 10.40 (d, 4H, ^3J = 9.6 Hz, H^b), 9.16 (d, 4H, ^3J = 9.3 Hz, H^a), 8.87 (m, 2H, H$_{Ar}$), 7.33 (m, 2H, H$_{Ar}$), 7.20 (m, 2H, H$_{Ar}$). ^{13}C NMR (150.92 MHz, TFA-d_1, 295 K) δ 170.6 (dd, $^1J_{CF}$ = 264.4 Hz, $^3J_{CF}$ = 14.5 Hz, C11), 164.8 (dd, $^1J_{CF}$ = 255.4 Hz, $^3J_{CF}$ = 13.5 Hz, C9), 155.1 (C7), 153.9 (C6), 140.3 (C4H^b), 137.4 (d, $^3J_{CF}$ = 10.7 Hz, C13H$_{Ar}$), 132.1 (C3), 128.9 (C5H^a), 123.0 (C2), 116.6 (dd, $^2J_{CF}$ = 22.7 Hz, $^4J_{CF}$ = 2.7 Hz, C12H$_{Ar}$), 116.4 (dd, $^2J_{CF}$ = 9.0 Hz, $^4J_{CF}$ = 3.4 Hz, C8), 116.2 (C1), 107.7 (t, $^2J_{CF}$ = 26.6 Hz, C10H$_{Ar}$). HRMS (EI): m/z calcd for $C_{34}H_{14}N_4F_4$ 554.1155,

found 554.1163. Anal. Calcd for $C_{34}H_{14}N_4F_4$: C 73.65, H 2.54, N 10.10. Found: C 73.92, H 2.65, N 10.18.

2,9-Bis(2,4,5-trifluoro-phenyl)-1,3,8,10-tetraazaperopyrene (6d). Acid chloride: 2,4,5-trifluorobenzoyl chloride. Yield: 432 mg (0.7 mmol; 73%) of **6d** as an orange powder. ^{1}H NMR (600.13 MHz, TFA-d_1) δ 10.57 (d, 4H, ^3J = 9.7 Hz, H^b), 9.33 (d, 4H, ^3J = 9.3 Hz, H^a), 8.84 (m, 2H, H_{Ar}), 7.48 (m, 2H, H_{Ar}). ^{13}C NMR (150.92 MHz, TFA-d_1, 295 K) δ 160.0 (dd, $^1J_{CF}$ = 252.6 Hz, $^3J_{CF}$ = 10.5 Hz, C9), 158.9 (C7), 157.9 (m, C11), 153.9 (C6), 151.0 (m, C12), 140.5 (C4), 132.2 (C3), 128.9 (C5), 123.6 (C2), 122.9 (C13H_{Ar}), 116.5 (C8), 116.3 (C1), 110.3 (C10H_{Ar}). HRMS (EI): m/z calcd for $C_{34}H_{12}N_4F_6$ 590.0966, found 590.0929. Anal. Calcd for $C_{34}H_{12}N_4F_6$ (590.5): C 69.16 H 2.05 N 9.49. Found: C 68.86 H 2.23 N 9.48.

2,9-Bis(3,5-difluoro-phenyl)-1,3,8,10-tetraazapero-pyrene (6e). Acid chloride: 3,5-difluorobenzoyl chloride. Yield: 400 mg (0.7 mmol; 72%) of **6e** as an orange powder. ^{1}H NMR (600.13 MHz, TFA-d_1) δ 10.59 (d, 4H, ^3J = 9.7 Hz, H^b), 9.35 (d, 4H, ^3J = 9.3 Hz, H^a), 8.37 (m, 4H, H_{Ar}), 7.42 (m, 2H, H_{Ar}). ^{13}C NMR (150.92 MHz, TFA-d_1, 295 K) δ 166.7 (dd, $^1J_{CF}$ = 252.9 Hz, $^3J_{CF}$ = 12.4 Hz, C10), 157.0 (t, $^4J_{CF}$ = 3.3 Hz, C7), 154.3 (C6), 140.4 (C4), 135.0 (t, $^3J_{CF}$ = 9.8 Hz, C8), 132.1 (C3), 128.9 (C5), 123.0 (C2), 116.5 (C1), 114.7 (dd, $^2J_{CF}$ = 21.8 Hz, $^4J_{CF}$ = 6.9 Hz, C9H_{Ar}), 112.4 (t, $^2J_{CF}$ = 25.3 Hz, C11H_{Ar}). HRMS (EI): m/z calcd for $C_{34}H_{14}N_4F_4$ 554.1155, found 554.1140. Anal. Calcd for $C_{34}H_{14}N_4F_4$: C 73.65 H 2.54 N 10.10. Found: C 73.36 H 2.78 N 10.09.

2,9-Bis(4-bromo-2-fluoro-phenyl)-1,3,8,10-tetraazaperopyr-ene (7a). Acid chloride: 4-bromo-2-fluorobenzoyl chloride. Yield: 300 mg (0.4 mmol; 44%) of **7a** as an orange powder. ^{1}H NMR (600.13 MHz, TFA-d_1) δ 10.50 (d, 4H, ^3J = 9.4 Hz, H^b), 9.26 (d, 4H, ^3J = 9.3 Hz, H^a), 8.77 (m, 2H, H_{Ar}), 7.85 (m, 2H, H_{Ar}), 7.76 (m, 2H, H_{Ar}). ^{13}C NMR (150.92 MHz, TFA-d_1, 295 K) δ 164.0 (C7), 162.4 (C9), 155.1 (d, $^1J_{CF}$ = Hz, C9F), 153.8 (C6), 140.2 (C4), 135.7 (t, C10), 132.0 (C3), 131.3 (C12), 128.5 (C5), 123.1 (C2), 122.9 (C13H_{Ar}), 118.6 (C11Br), 116.2 (C1). HRMS (EI): m/z calcd for $C_{34}H_{14}N_4{}^{79}Br_2F_2$ 673.9553, found 673.9557. Anal. Calcd for $C_{34}H_{14}N_4Br_2F_2$: C 60.38 H 2.09 N 8.28. Found: C 60.74 H 2.32 N 8.37.

2,9-Bis(4-bromo-2,3,5,6-tetrafluoro-phenyl)-1,3,8,10-tetra-azaperopyrene (7b). Acid chloride: 4-bromo-2,3,5,6-tetrafluoro-benzoyl chloride. Yield: 365 mg (0.2 mmol; 47%) of **7b** as an orange powder. ^{1}H NMR (600.13 MHz, TFA-d_1) δ 10.67 (d, 4H, ^3J = 9.4 Hz, H^b), 9.38 (d, 4H, ^3J = 9.1 Hz, H^a). ^{13}C NMR (150.92 MHz, TFA-d_1, 295 K) δ 163.8 (C7), 154.0 (d, C6), 140.7 (C4), 132.4 (C3), 128.9 (C5), 122.7 (C2), 122.9 (C13H_{Ar}), 116.5 (C1). HRMS (EI): m/z calcd for $C_{34}H_8N_4{}^{79}Br_2F_8$ 781.8988, found 781.9051. Anal. Calcd for $C_{34}H_8N_4Br_2F_8$: C 52.08 H 1.03 N 7.14. Found: C 52.55 H 1.21 N 7.08.

X-ray Crystal Structure Determinations. Crystal Data. Data for 3: $C_{36}H_{16}F_6N_4$, monoclinic, $P2_1/n$, a = 10.2372(9), b = 7.3908(7), c = 34.902(3) Å, β = 93.567(2)°, V = 2635.6(4) Å^3, Z = 4, μ = 0.123 mm^{-1}, F_{000} = 1256. T = 100(2) K, θ range 2.0−25.0°. Index ranges h, k, l (indep set): −12−12, 0−8, 0−41. Reflections measd: 42526, indep: 4651 [R_{int} = 0.0761], obsvd [$I > 2\sigma(I)$]: 3206. Final R indices [$F_o > 4\sigma(F_o)$]: $R(F)$ = 0.0583, $wR(F^2)$ = 0.1379, GOF = 1.056.

Data for 6a: $C_{34}H_8F_{10}N_4$, monoclinic, $P2_1/n$, a = 11.602(4), b = 3.7260(13), c = 28.062(10) Å, β = 96.652(6) °, V = 1204.9(7) Å^3, Z = 2, μ = 0.164 mm^{-1}, F_{000} = 660. T = 100(2) K, θ range 2.0 to 27.5°. Index ranges h, k, l (indep set): −15−14, 0−4, 0−36. Reflections measd: 23373, indep: 2754 [R_{int} = 0.057], obsvd [$I > 2\sigma(I)$]: 1774. Final R indices [$F_o > 4\sigma(F_o)$]: $R(F)$ = 0.0808, $wR(F^2)$ = 0.1366, GOF = 1.017.

Data for 6b: $C_{34}H_{14}F_4N_4$, triclinic, P-1, a = 6.9689(4), b = 10.5536(7), c = 16.8584(10) Å, α = 82.549(1), β = 86.086(1), γ = 73.071(1) °, V = 1175.5(1) Å^3, Z = 2, μ = 0.116 mm^{-1}, F_{000} = 564. T = 100(2) K, θ range 2.0 to 31.0°. Index ranges h, k, l (indep set): −10−10, −15−15, 0−24. Reflections measd: 29190, indep: 7427 [R_{int} = 0.0469], obsvd [$I > 2\sigma(I)$]: 4731. Final R indices [$F_o > 4\sigma(F_o)$]: $R(F)$ = 0.0505, $wR(F^2)$ = 0.1299, GOF = 1.046.

Data for 7b: $C_{34}H_8Br_2F_8N_4$, monoclinic, $P2_1/c$, a = 3.7285(18), b = 30.356(15), c = 11.801(6) Å, β = 93.334(9)°, V = 1333(1) Å^3, Z = 2, μ = 3.133 mm^{-1}, F_{000} = 764. T = 100(2) K, θ range 1.9 to 26.4°. Index ranges h, k, l (indep set): −4−4, 0−37, 0−14. Reflections measd: 23953, indep: 2742 [R_{int} = 0.068], obsvd [$I > 2\sigma(I)$]: 2387. Final R indices [$F_o > 4\sigma(F_o)$]: $R(F)$ = 0.0895, $wR(F^2)$ = 0.2146, GOF = 1.227.

Data for H_26a^{2+}: $C_{50}H_{16}F_{34}N_4O_{16}$, triclinic, P-1, a = 7.985(4), b = 11.766(6), c = 16.176(8) Å, α = 80.477(11), β = 79.834(9), γ = 74.240(8) °, V = 1428(1) Å^3, Z = 1, μ = 0.205 mm^{-1}, F_{000} = 778. T = 100(2) K, θ range 2.1 to 26.4°. Index ranges h, k, l (indep set): −9−9, −14−14, 0−20. Reflections measd: 42448, indep: 7606 [R_{int} = 0.0747], obsvd [$I > 2\sigma(I)$]: 4540. Final R indices [$F_o > 4\sigma(F_o)$]: $R(F)$ = 0.0806, $wR(F^2)$ = 0.1548, GOF = 1.031. The crystal was an approximately 1:1 twin. Singles and composites that include domain 1 were used for refinement.

Intensity data were collected at low temperature (Bruker AXS Smart 1000 CCD diffractometer, Mo Kα radiation, graphite monochromator, λ = 0.71073 Å) and corrected for Lorentz, polarization, and absorption effects (semiempirical).[23,24] Structure solution: conventional direct methods (**3**, H_2**6a**$^{2+}$),[25,26] direct methods with dual-space recycling (**6a**, **6b**),[27] heavy atom method combined with structure expansion by direct methods.[28] Refinement: full-matrix least-squares methods based on F^2;[25] all non-hydrogen atoms anisotropic, hydrogen atoms taken from Fourier maps or at calculated positions (refined fully or riding). Distance and adp restraints were applied to disordered groups.

Acknowledgment. Financial support from the University of Heidelberg, the Doctoral College "Molekulare Sonden" is gratefully acknowledged. We also thank the German Ministry of Education and Research (BMBF) for this work within the project POLYTOS (FKZ: 13N10205) in the Research Network "Forum Organic Electronics" for funding.

Supporting Information Available: General experimental methods; compound characterization by ^{1}H and ^{13}C NMR spectra for all compounds; computational, cyclovoltammetric, and X-ray crystallographic data. This material is available free of charge via the Internet at http://pubs.acs.org.

(23) Blessing, R. H. *Acta Crystallogr.* **1995**, *A51*, 33–38.
(24) Sheldrick, G. M. *SADABS*; Bruker AXS: Madison, WI, 2004−2008. Sheldrick, G. M. *TWINABS*; Bruker AXS: Madison, WI, 2004−2008.
(25) Sheldrick, G. M. *SHELXS-97*; University of Göttingen: Germany, 1997.
(26) Sheldrick, G. M. *Acta Crystallogr.* **2008**, *A64*, 112–122.
(27) (a) Burla, M. C.; Caliandro, R.; Camalli, M.; Carrozzini, B.; Cascarano, G. L.; De Caro, L.; Giacovazzo, C.; Polidori, G.; Spagna, R. *J. Appl. Crystallogr.* **2005**, *38*, 381–388. (b) Burla, M. C.; Caliandro, R.; Camalli, M.; Carrozzini, B.; Cascarano, G. L.; De Caro, L.; Giacovazzo, C.; Polidori, G.; Spagna, R. *SIR2004*; CNR IC: Bari, Italy, 2004.
(28) (a) Beurskens, P. T. In Sheldrick, G. M., Krüger, C., Goddard, R., Eds.; *Crystallographic Computing 3*; Clarendon Press: Oxford, U.K., 1985; p 216. (b) Beurskens, P. T.; Beurskens, G.; de Gelder, R.; Smits, J. M. M., Garcia-Granda, S.; Gould, R. O. *DIRDIF-2008*; Radboud University Nijmegen: The Netherlands, 2008.